Supplementary Information (SI) for RSC Sustainability.

Supplementary Material

PRODUCTION OF MAGNESIUM FERRITE FOR USE AS PHOSPHATE ADSORBENTS IN WATER

Matheus Henrique Pimentel Araújo[a]*, Laura Melo Fernandes Moreira[a], José Domingos Ardisson[b], Rochel Monteiro Lago[c], Juliana Cristina Tristão[a]*

Mössbauer spectroscopy

Table S 1: Hyperfine parameters obtained at 23K for samples MgFe, MgFe300, MgFe700, and MgFe900.

Sample	Phase		δ (± 0.05) (mm s^{-1})	ε (± 0.05) (mm s^{-1})	B_{HF} (± 0.5) (T)	AR (±1) (%)
MgFe	α-Fe_2O_3		0.48	-0.18	52.7	60
	Fe^{3+}		0.48	-0.21	51.3	40
MgFe300	α-Fe_2O_3		0.47	-0.18	53.4	74
	Fe^{3+}		0.47	-0.21	52.1	26
MgFe700	$MgFe_2O_4$	Octa	0.37	-0.08	52.2	31
		Tetra	0.34	-0.03	49.9	31
	α-Fe_2O_3		0.47	-0.18	53.4	38
MgFe900	$MgFe_2O_4$	Octa	0.46	-0.04	51.3	35
		Tetra	0.35	-0.08	50.9	27
	α-Fe_2O_3		0.47	0.10	53.7	38

δ = isomeric shift for α-Fe; ε = quadrupolar shift; BHF = hyperfine field; AR = relative spectral area

Vibrating sample magnetometer (VSM)

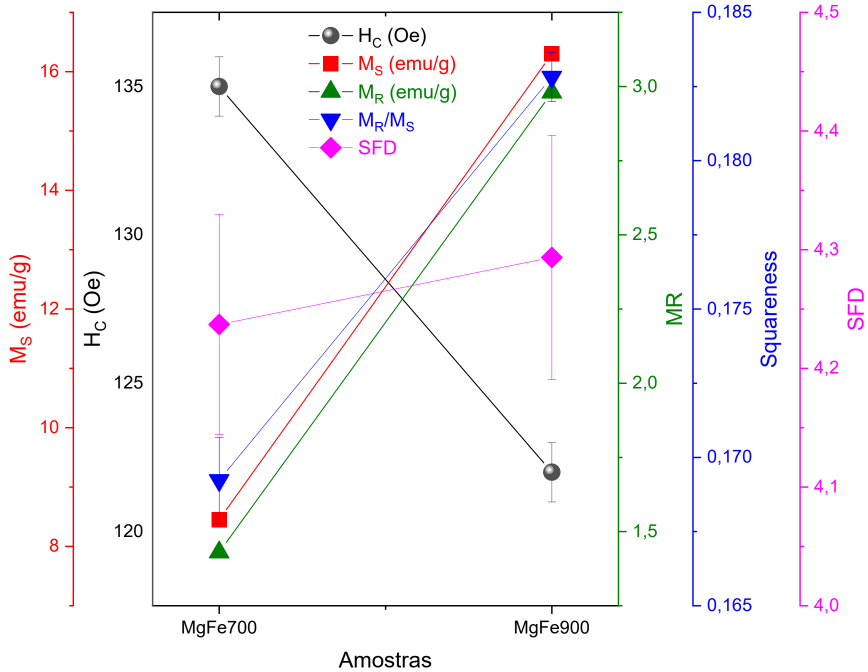

S 1: Magnetic property values for the MgFe700 and MgFe900 samples obtained from the hysteresis curve. For this image, Hc, Mr, Ms, Squareness, and SFD are respectively the field coherence, remanent magnetization, magnetic saturation, quadrature curve (S = Mr/Ms), and switching field distribution of the samples (SFD = switching field distribution).

Energy dispersive spectroscopy (EDS)

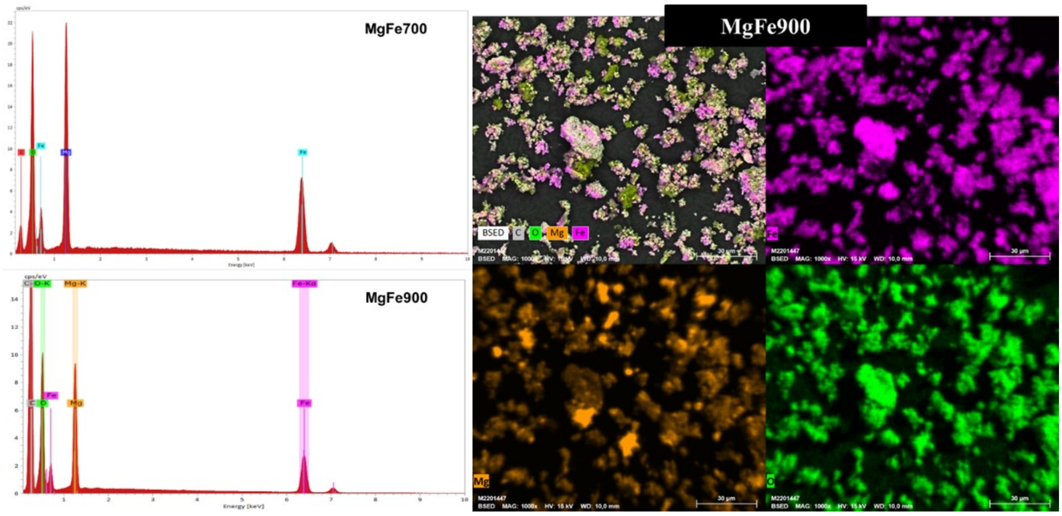

S 2: Energy dispersive X-ray spectra of MgFe700 and MgFe900 samples and chemical map obtained by energy dispersive X-rays and of the MgFe900 sample.

Determination of the adsorption capacity of PO_4^{3-}

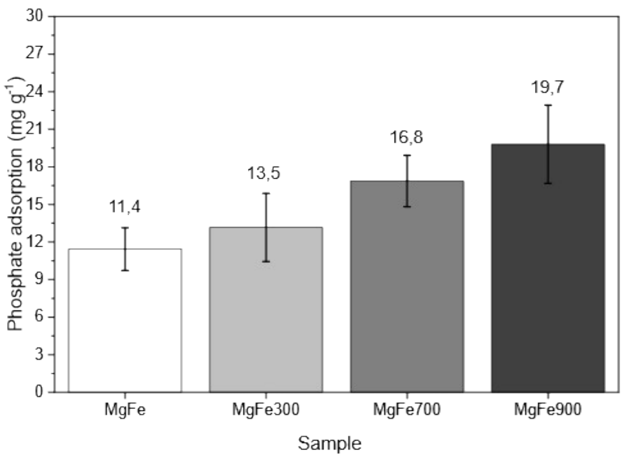

S 3: Phosphate adsorption capacity (50 mg L^{-1}) for samples MgFe, MgFe300, MgFe700 and MgFe900. (adsorbent dose: 1 g L^{-1}, 24 h, $[PO_4^{3-}]$ = 50 mg g^{-1},150 rpm).

Release of Fe and Mg during material washing

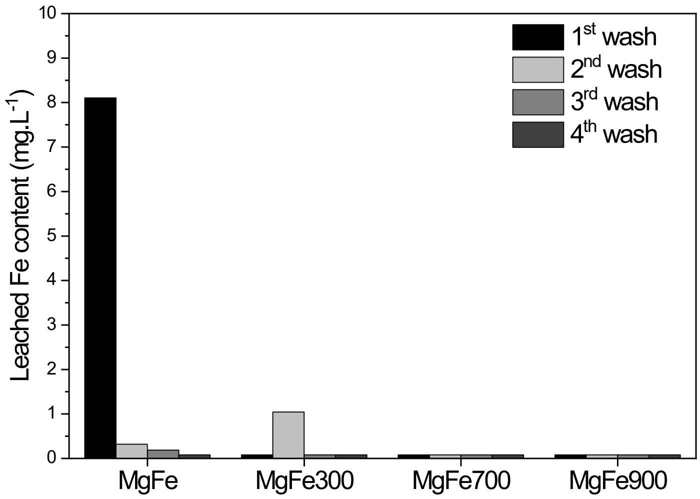

S 4: Iron (Fe) release according to the four washes in each material (MgFe, MgFe300, MgFe700, MgFe900).

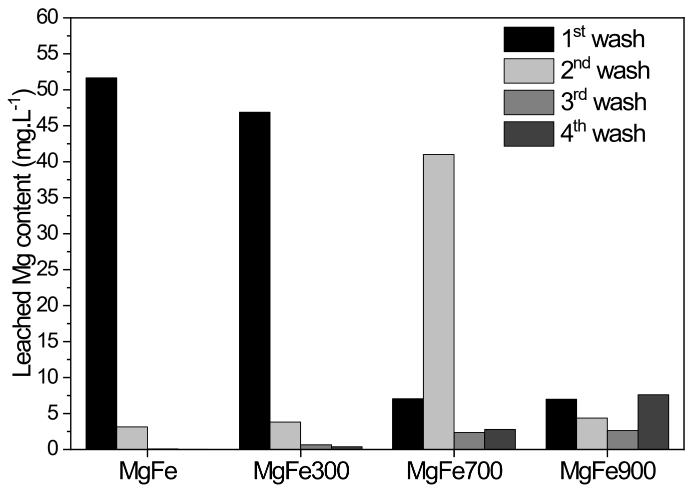

S 5: Magnesium (Mg) release according to the four washes in each material (MgFe, MgFe300, MgFe700, MgFe900).

N_2 adsorption/desorption curve and the BET superficial area

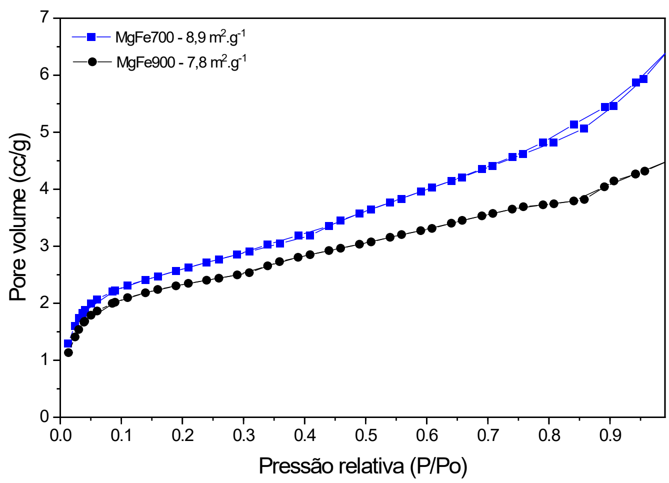

S 6: N_2 adsorption/desorption curve for MgFe700 and MgFe900 samples.

Infrared

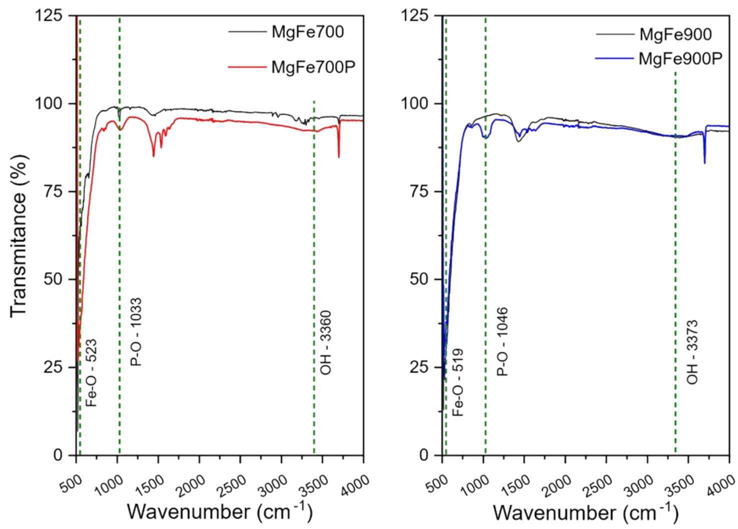

S 7: Absorption spectra in the infrared region (4000 - 500 cm^{-1}) for the MgFe700 and MgFe900 samples before and after adsorption.

Isotherm

Table S 2: Nonlinear equations for isotherm models.

Isotherm model		Equation	Reference
Two-parameters isotherm	*Langmuir*	$q_e = \dfrac{q_{max}K_L C_e}{1 + K_L C_e}$	[1–4]
	Freundlich	$q_e = K_F C_e^n$	
	Temkin	$q_e = B\ lnA_T C_e$	
Three-parameter isotherm	*Redlich–Peterson*	$q_e = \dfrac{K_R C_e}{1 + a_R C_e^n}$	

Kinetics

Table S 3: Nonlinear equations for kinetic models.

Kinetic model	Equation	Reference
Pseudo-first order	$q_t = q_e(1 - \varepsilon^{-kt})$	[5–10]
Pseudo-second order	$q_t = \dfrac{k_2 q_e^2 t}{1 + k_2 q_e t}$	
Elovich	$q_t = \dfrac{1}{\beta}\ln(1 + \alpha\beta t)$	

Zero point of charge (pH_{PZC})

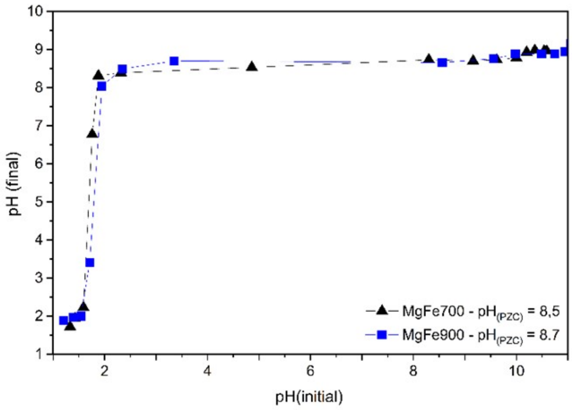

S 8: Zero point of charge (pH_{PZC}) values determined for samples MgFe700 and MgFe900.

Mg leaching under phosphate adsorption conditions

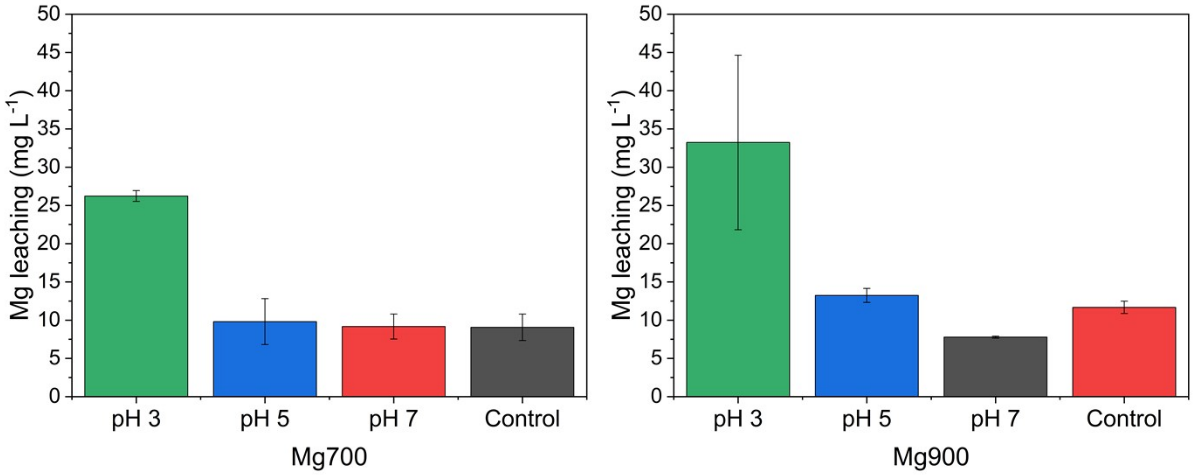

S 9: Concentration of leached Magnesium (Mg^{2+} - in mg L^{-1}) as a function of the initial pH of the solution (3, 5 and 7), in the presence of 50 mg L^{-1} of phosphate, for the materials MgFe700 and MgFe900.

Fe leaching under phosphate adsorption conditions

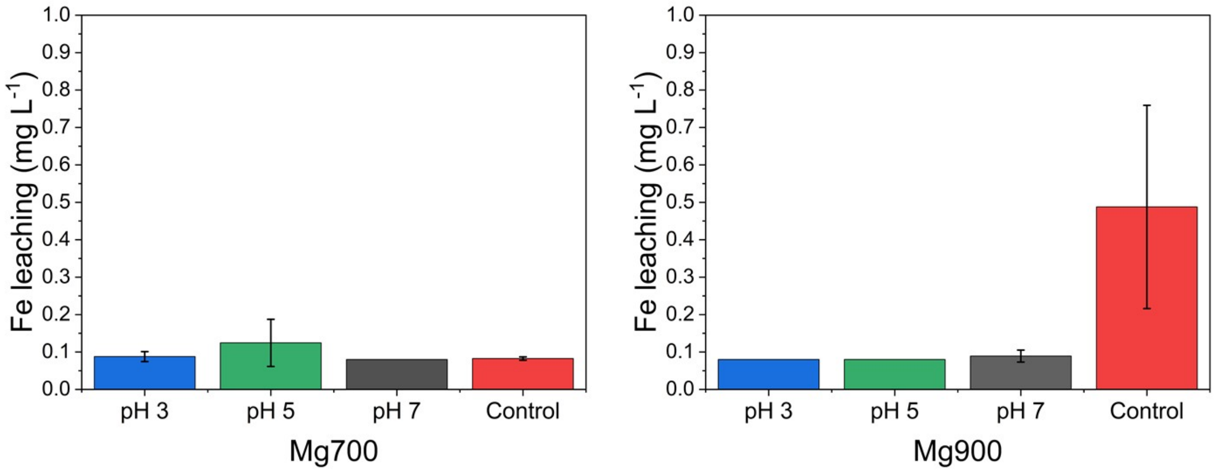

S 10: Concentration of leached Iron (Fe^{3+} - in mg L^{-1}) as a function of the initial pH of the solution (3, 5 and 7), in the presence of 50 mg L^{-1} of phosphate, for the materials MgFe700 and MgFe900.

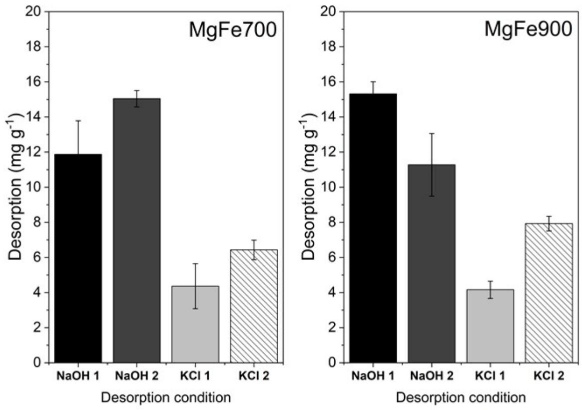

S 11: Phosphate desorption capacity (mg g^{-1}) using NaOH 0.5 mol L^{-1} (NaOH 1), NaOH 1 mol L^{-1} (NaOH 2), 0.01 mol L^{-1} (KCl 1), and 0.1 mol L^{-1} (KCl 2) for MgFe700 and MgFe900.

References

1 K. Y. Foo and B. H. Hameed, 2010, preprint, DOI: 10.1016/j.cej.2009.09.013.

2 N. Ayawei, A. N. Ebelegi and D. Wankasi, *Hindawi Limited*, 2017, preprint, DOI: 10.1155/2017/3039817.

3 C. R. Girish, *Article ID: IJCIET_08_10_010 International Journal of Civil Engineering and Technology*, 2017, 8, 80–86.

4 D. L. Peterson, *A USEFUL ADSORPTION ISOTHERM*, 1945, vol. 63.

5 L. Largitte and R. Pasquier, *Chemical Engineering Research and Design*, 2016, 109, 495–504.

6 R.-S. Juang and M.-L. Chen, *Ind Eng Chem Res*, 1997, 36, 813–820.

7 S. S. Ray, R. Gusain and N. Kumar, in *Carbon Nanomaterial-Based Adsorbents for Water Purification*, Elsevier, 2020, pp. 101–118.

8 L. Largitte and R. Pasquier, *Chemical Engineering Research and Design*, 2016, 109, 495–504.

9 M. Musah, Y. Azeh, J. Mathew, M. Umar, Z. Abdulhamid and A. Muhammad, *Caliphate Journal of Science and Technology*, 2022, 4, 20–26.

10 F. C. Wu, R. L. Tseng and R. S. Juang, *Chemical Engineering Journal*, 2009, 150, 366–373.